Contents lists available at ScienceDirect

Catena

Assessment of the soil water content in the Pampas region using SWAT

S.B. Havrylenko [a], J.M. Bodoque [b], R. Srinivasan [c], G.V. Zucarelli [d], P. Mercuri [a]

[a] *Instituto de Clima y Agua, CIRN-CNIA, INTA, Los Reseros y Las Cabañas s/n- B1686IQN, Hurlingham, Buenos Aires, Argentina*
[b] *Mining and Geological Engineering Department, University of Castilla La Mancha, Campus Fábrica de Armas, Avda. Carlos III, Toledo E-5071, Spain*
[c] *Spatial Sciences Laboratory in the Department of Ecosystem Science and Management, Texas A&M University, College Station, TX 77845, USA*
[d] *Facultad de Ingeniería y Ciencias Hídricas (FICH), UNL, Ciudad Universitaria, Paraje "El Pozo", 3000 Santa Fe, Argentina*

ARTICLE INFO

ABSTRACT

The Pampas region has recently experienced an expansion of agriculture towards more fragile environments, which has been associated with an increase in the frequency of droughts affecting the whole region. In the present study, we obtained a long-term record of soil water content (SWC) using a Soil and Water Assessment Tool (SWAT) model, for the first time in Argentina. The reliability of this model was contrasted with the temporal variation of the Standard Precipitation Index (SPI) and the Normalized Difference Vegetation Index (NDVI) to characterise episodes of drought. We also estimated the correlation between SWC anomaly (aSWC) and SPI, as well as the correlation between NDVI anomaly (aNDVI) and SPI. The model performance was reasonably satisfactory. The model calibration showed determination coefficient (R^2) and Nash–Sutcliffe coefficient (NS) values of 0.70 and 0.59, respectively, and the model validation showed R^2 and NS values of 0.77 and 0.75, respectively. The aNDVI showed a relatively low correlation with aSWC ($0.26 \leq r \leq 0.45$). In contrast, the SPI presented significantly positive correlations with aSWC ($0.67 \leq r \leq 0.83$). This work showed that SWAT is a suitable tool to measure SWC in poorly gauged geographical areas such as the Pampas region. Additionally, our approach could be applied to other systems resembling that studied here, without any significant reduction in performance.

© 2015 Elsevier B.V. All rights reserved.

1. Introduction

Droughts are a natural hazard occurring in almost all regions of the world (Das et al., 2003; Van Lanen et al., 2013; Wilhite et al., 2014), with an intensity and frequency of occurrence which depend on each region (Ravelo et al., 1999). Drought is considered to be a slow and complex phenomenon affecting large regions, and its severity is difficult to determine (Wilhite, 2005). More specifically, agricultural droughts (Narasimhan and Srinivasan, 2005) can frequently occur along different phenological periods of the crop, affecting different areas and generating significant production losses (Xu et al., 2013). Argentine agricultural sector has shown an important expansion since the early seventies, with an increase in the nineties (Viglizzo, 2008). This process has extended the agricultural frontier into more fragile environments and it has replaced traditional crops, pastures and native forests for soy monocultures (Viglizzo et al., 2001), leaving these new production areas more exposed to water-related hazards (i.e. droughts or floods).

In Argentina, diverse approaches have been applied to characterise agricultural droughts at regional scales. Researchers as Núñez et al. (2005), Seiler and Rotondo (2006) and Gonzalez and Cariaga (2009) applied the Standard Precipitation Index (SPI, McKee et al., 1993) to characterise droughts in large areas of the Pampas region. The SPI

index is recommended because of its simplicity and flexibility for identifying and monitoring wet and dry events at various temporal scales. Moreover, Llano and Penalba (2010) studied some characteristics of dry sequences using daily precipitation data, to analyse the degree of spatial coherence and the temporal variability of these sequences throughout Argentina. In addition, some authors explored remote sensing techniques to assess the impact of agricultural droughts on crop yields. For example, Seiler et al. (1998), Ravelo et al. (1999), and Hartmann et al. (2003) applied indices for using themas indicators of drought derived from remote sensing data (e.g. SPOT-Vegetation, Normalized Difference Vegetation Index (NDVI), Vegetation Condition Index (VCI), etc.). They found that satellite data can provide valuable information about drought development, impacts, and also about crop condition and production at regional scale. However, to date, no studies have determined soil water content (SWC) as an indicator able to characterise agricultural droughts in Argentina at the basin level.

SWC in the root zone (Maltese et al., 2013) is an excellent indicator of agricultural drought (Johnson et al., 2009), as it is a measure that depends on weather variables (e.g. precipitation and evapotranspiration), soil properties (e.g. water storage capacity, texture, structure), existing vegetation, and management practices (Narasimhan et al., 2005). SWC is also an important hydrological parameter that controls various processes of the hydrological cycle. Additionally, on the ground surface, soil moisture is a critical factor in the interaction with the atmosphere, while in the root zone, it conditions the coverage and state of vegetation

(Schnur et al., 2010). Researchers such as Mavi and Tupper (2004), Wilhite (2005), Mishra et al. (2009), Hong et al. (2010), and Han et al. (2012) concluded that, in order to characterise SWC, hydrological modelling should be combined with other approaches.

Numerous hydrological models have proved useful for modelling spatial and temporal distribution of soil moisture at basin level (Bergström, 1995; Liang et al., 1996; Grayson et al., 1997; Zhang et al., 1999; Klawitter, 2006). Among the many hydrological models currently available, Soil and Water Assessment Tool (SWAT), developed by USDA Agricultural Research Service (ARS) (Arnold and Fohrer, 2005; Neitsch et al., 2011), was chosen for this research to specifically determine its reliability to calculate SWC in the Pampas region. SWAT has been extensively used by researchers since it has been designed to predict the impact of land management practices on water, sediment and agricultural management planning of large and complex watersheds.

Narasimhan and Srinivasan (2005), Li et al. (2010), Richard et al. (2010), and Wang et al. (2011) have used SWAT as a suitable model to simulate SWC at sub-basin level. These authors have successfully implemented SWAT to simulate SWC in different basins and regions. They found that SWAT can generate long-term SWC series, and they also compared the simulated data with observed data as well as those coming from other sources, such as SPI and NDVI. Nevertheless, the application of SWAT in regions as Argentina, where there are few hydrological data, is a challenge, given that SWAT requires a diversity of spatially distributed information in order to run adequately (e.g. accurate topography, land uses, soils) together with many inputs, necessary for proper calibration. Furthermore, very little hydrological modelling has been made using SWAT model in Argentina, which creates the opportunity to explore its use as a new tool.

This study provides an approach to assess droughts in watersheds with agricultural activity and to monitor the impacts of drought on soil moisture, growth and crop yield at basin level. The main aim was to explore the reliability of the SWAT model to estimate SWC in a poorly gauged basin of the Pampas region with specific drought indicators, such as NDVI and SPI. The specific objectives were: (1) to develop a long-term record of SWC using SWAT; (2) to analyse the correlation between SWC anomaly (aSWC) and SPI as well as the correlation between NDVI anomaly (aNDVI) and aSWC; (3) to analyse the temporal variability of NDVI, SPI and SWC.

2. Material and methods

2.1. Study area

The Arrecifes basin is located in the centre of the Pampas region (north of Buenos Aires province) (Fig. 1), covering an area of 10,700 km². The outlet of the study area coincides with the gauging station "Arrecifes" defining a draining area of 8742 km² (Fig. 1). This basin belongs to the Rolling Pampa region. The topography is characterised by the presence of low round-topped hills, which gives the landscape a rolling geomorphology. The elevation ranges from 21 m at the basin outlet to 108 m at the highest point in the catchment. The basin has a high drainage density, being 176.9 km its longest flow path.

The Arrecifes river has a flow regime module of 21 m³/s with an average annual contribution of 579 Hm³/year. Based on the flow time series available, it can be observed that the hydrological regime exhibits flow peaks during spring and autumn, which coincide with the period of greatest rainfall (September to May). Conversely, minimum flows take place during late winter and January, corresponding to the month with greatest water deficit.

This watershed has a particular interest for agricultural activities because it is located in the humid Pampas region (Fig. 1), the most productive ecoregion of the country (National Institute of Agricultural Technology of Argentina (INTA), 2009). In this zone, the soils are very deep, neither alkaline nor saline, with a moderate susceptibility to water erosion and a good agricultural potential. According to the Köppen–Geiger climate map (Peel et al., 2007), temperate rain is the dominant climate, Cfa called "humid subtropical climate".

The basin has an average winter temperature of 11 °C, while the average summer temperature is 23 °C (Bianchi and Cravero, 2010).
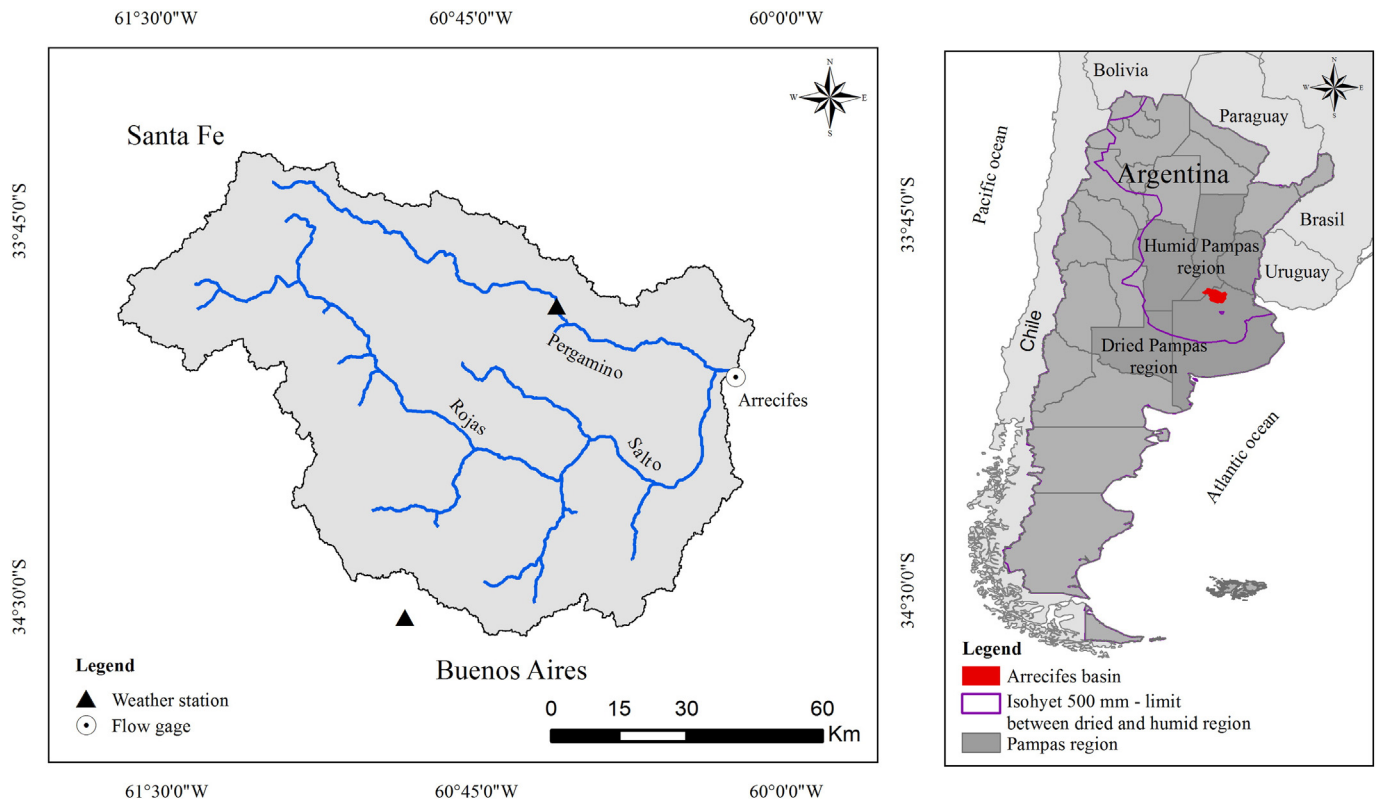
Fig. 1. Location of the study area.

Annual precipitation presents no spatially marked gradient and it ranges from 1000 to 1200 mm. Further, maxima precipitation occurs in spring and autumn and is mainly generated from convective phenomena. Usually, these storms are local, presenting large spatial variability, while minimum precipitations occur in winter, associated with frontal systems. However, the water deficit of greatest importance occurs during late spring and early summer, as a result of increased evapotranspiration at this time of the year. The annual potential evapotranspiration of the region ranges from 1000 to 1200 mm, with maxima monthly values up to 160 mm in January (INTA, 2013).

2.2. Input data

The data required to apply the SWAT model were gathered from various sources and subjected to appropriate processing before being incorporated into the model. Daily meteorological data were obtained from two weather stations (Fig. 1). The time series taken into account for the simulation was between 1959 and 2011. We checked the quality of the data using stationarity and independence of the data as criteria. To do this, the non-parametrical Mann–Kendall (Hirsch et al., 1982) test was used for trend analysis, while Kolmogorov–Smirnov (Conover, 1999) test was chosen to assess the continuity of data. Also, we graphically analysed the time series to detect invalid and missing values.

Topographic data (Table 1) were derived from the C Band corresponding to the Shuttle Radar Topography Mission (SRTM-C) of 1 arc second resolution (Farr et al., 2007). However, SRTM data cannot be directly used for hydrological applications. This is because band C signal is especially sensitive to the geometry and orientation of the vegetation leaves. Therefore, the energy is strongly scattered, unable to penetrate the vegetation, so the resulting Digital Elevation Model (DEM) does not show the ground surface but the height of the visible surface, e.g. vegetation and buildings (Fig. 2A). In the Pampas region, the description above is denoted by a continuous mosaic of crops and grassland areas interrupted by small forests. These height peaks cause a significant source of noise, especially in flat areas as those in this study (Fig. 2B). As a result, the SRTM-C data had to be filtered by identifying and deleting pixels (arboreal and shrubby vegetation) which could lead to errors in the model (Fig. 2C). This process allowed us to obtain the ground surface topography and ensure that flow direction and flow accumulation algorithms (Olivera and Maidment, 1999) accurately reflected the hydrological network of the basin. Then, the gaps were filled using a multisurface interpolation technique (Wang, 1990). Lastly, to homogenize the surface of the DEM, we applied the median filter, which is a sliding-window spatial filter that replaces the centre value for the median of all the pixel values of the window (Fig. 2D).

Land use coverage (Fig. 3) was derived using an automatic object extraction technique from satellite images provided by the Landsat 5 Thematic Mapper (TM) sensor. Prior to their use, the scenes were geometrically corrected resorting to Landsat 7 ETM + images (Table 1) as basis. The automatic object extraction technique differs from the pixel-based classification because it generates highly accurate classification results, whereas pixel-based approaches often have 'salt-and-pepper' noise as they assume that the data of each pixel are independent (Blaschke, 2010; Susaki, 2012). First, we made a contextual segmentation where final segments (the objects) were depicted with a variety of spatial, spectral (brightness and colour), and texture attributes. These segments ideally correspond to real-world objects (Platt and Rapoza, 2008; Blaschke, 2010). Next, we applied a supervised classification approach where some of these objects were selected as training areas for the specified land use. Subsequently, all objects appearing in the images were classified so as to become the most representative for their land use. In order to establish results' quality, the final classification was visually interpreted (Haack and Jampoler, 1995; Horler and Ahern, 1986). Land use mapping was tested based on field observations and analysis from Google Earth Images.

Soil map (Fig. 4) was derived from soil cartography published by INTA (2009) at resolution of 1:50,000. The database contains major physical and chemical properties at unit series level. Each unit is composed for three subgroups that were classified according to the USDA Soil Taxonomy (Soil Survey Staff, 2014). In this research, only the predominant subgroup of each unit series was considered (Table 2). Additional soil parameters required by SWAT were calculated using the software Soil Water Characteristic (Saxton and Rawls, 2006) and other regional soil information (INTA, 2009). Finally, the subgroup soil information was used to generate the soil input file which was imported to the SWAT Database.

2.3. Hydrological modelling

SWAT is a continuous long-time, semi-distributed and physically based model. It can simulate different parameters at the spatial resolution necessary to capture the spatial variability of the watershed (Di Luzio and Arnold, 2004; Neitsch et al., 2011), requiring spatially distributed information in order to run. Simulation of the hydrological cycle of a watershed is divided into two parts: land phase and routing.

The land phase determines the amount of the loadings (i.e. water, sediments and nutrients). The water balance is simulated for each HRU and is represented by four storage volumes: snow, soil profile (0–2 m), shallow aquifer (typically 2–20 m), and deep aquifer. The model parameterization starts by dividing the watershed into subunits. This division is helpful when the basin reflects a large scale spatial heterogeneity to impact hydrology processes (Neitsch et al., 2011). In this study, this step was based on surface topography. The watershed was partitioned into 20 sub-basins, taking into account the homogeneity of soil series (Fig. 4). For this purpose, the stream network was built considered a minimum drainage area of 4398 ha. Afterwards,

Table 1
Remote sensing data used.

Sensor	Purpose	Data type	Spatial resolution	Path/row	Date acquired	Catalogue
Landsat 7 ETM +	Geometric correction	L1G	30 m	226-084	12/09/1999	University of Maryland (http://glcf.umd.edu/)
				226-083	11/28/2001	
				227-084	12/16/1999	
				227-083	04/22/2000	
Landsat 5 TM	Classification	Level 5	30 m	226-084/83	09/15/2006	National Commission of Spatial Activities
				226-084/83	12/04/2006	(http://catalogos.conae.gov.ar
				226-084/83	01/21/2007	/Landsat/)
				226-084/83	02/22/2007	Brazilian Institute for Space Research
				226-084/83	03/10/2007	(http://www.dgi.inpe.br/CDSR/).
				227-084/83	10/24/2006	
				227-084/83	12/27/2006	
				227-084/83	02/13/2007	
				227-084/83	03/17/2007	
SRTM	Topography	DTED-2	1″			National Geographic Institute (http://www.ign.gob.ar/)
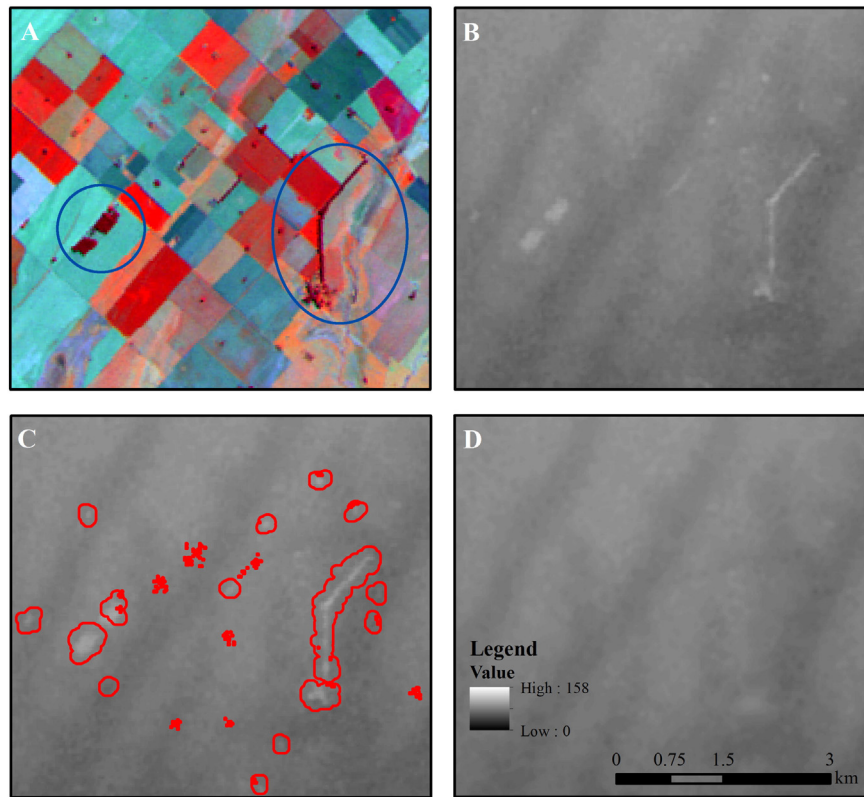
Fig. 2. A) False colour composite of a multispectral Landsat 5 TM image (R:4, G:5, B:3). Arboreal masses appear in blue shapes in dark red; B) SRTM-C data without filter. Whiter shades correspond to elevated surfaces due to tree vegetation; C) red shapes represent heights not linked to ground surface; D) final SRTM-C data once it was filtered. (For interpretation of the references to colour in this figure legend, the reader is referred to the web version of this article.)
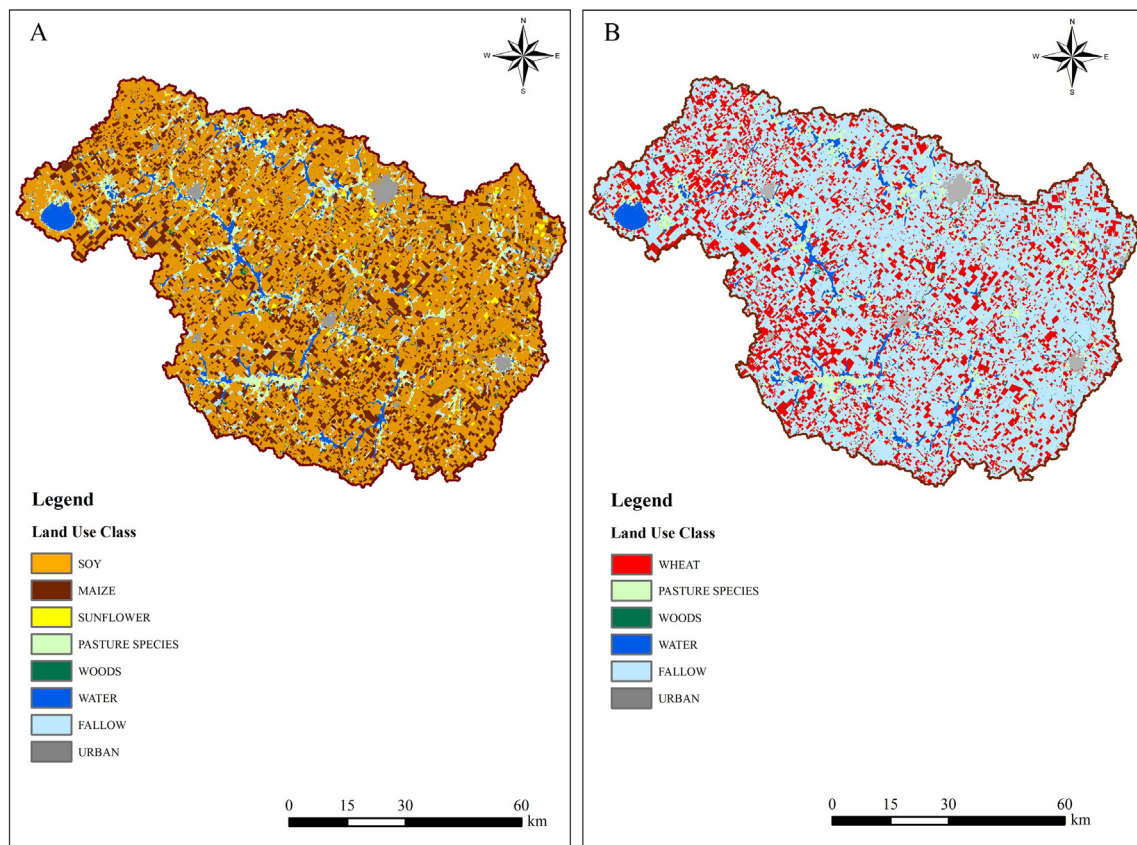
Fig. 3. Land uses maps: A) summer crops; B) winter crops.
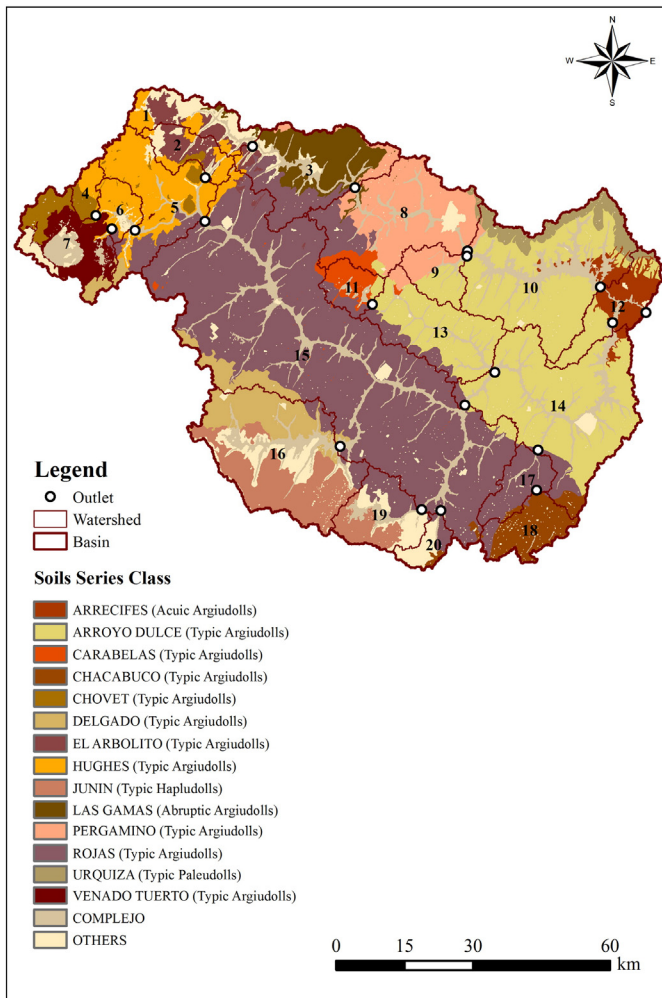
Fig. 4. Soil map of the Arrecifes basin.

sub-watersheds were delineated redefining the position of outlets in order to coincide with the boundaries of soil series (Fig. 4).

Once the above corrections were made, the sub-basins were discretised into a series of hydrologic response units (HRUs), which are portions that present a unique soil type, land use and management combination (Arnold et al., 2011). Runoff is predicted separately for each HRU and routed to the associated reach and catchment outlet through the channel network to obtain the total runoff for the watershed (Neitsch et al., 2011). In total, 337 HRUs were delineated by the

definition of a 2% level threshold for land use, 5% for soil type, and a uniform slope to decrease the computational time.

Subsequently, the physical characteristics of the hydrological network and the sub-basin geomorphology were automatically estimated from the DEM by the model. However, due to the low spatial resolution of this one (i.e. 30 m), some values were corrected to the best of our possibilities, resorting to cross-sections provided by the National Water Institute of Argentina (INA). Two 5-km-long reaches corresponding to the main channel were used and Google Earth was referred to the remaining reaches.

The growth cycle of a plant is controlled by plant attributes and management operations (Neitsch et al., 2011).Rainfed crops were considered in the entire basin assuming a classical crop rotation. The planting rotation was aimed to simulate the evolution of land use based on three short-term (3 years) scenarios of different vegetation covers. The crop rotation system was taken from the guides of field crops of Argentina provided by INTA and Rural Change Program (PCR) (1997a, b,c,d). The schedule was defined by calendar day and for each crop. Management operations (Table 3) were listed in chronological order and only one land cover could grow in each HRU at a time, i.e. before planting a new crop the previous land cover had to be removed.

Finally, the method chosen to estimate potential evapotranspiration (PET) was Priestley–Taylor (Priestley and Taylor, 1972). This method is appropriate to be used when detailed meteorological measurements are not available. In this regard, Priestley–Taylor does not require wind speed data, which is a local variable that changes significantly in time and space. Additionally, the CN parameter was calculated as function of plant evapotranspiration, since this method is less dependent on soil storage and more dependent on antecedent climate (Neitsch et al., 2011).

In the routing phase, the loadings were routed through the stream network channel of the watershed. Flow was moved by using a variable storage coefficient method developed by William (1969). As a final stage, the simulation was conducted using a monthly time step, beginning on January 1, 1969 and ending on December 31, 2002. The first 6 years (1969–1974) were used as warm-up period to mitigate the unknown initial conditions and were excluded from the analysis.

2.4. Model performance evaluation

Model performance was assessed using SWAT-CUP. This programme includes five methods from which the Sequential Uncertainty Fitting was chosen (SUFI-2) (Abbaspour et al., 2004, 2007, Schuol et al., 2008). Daily discharge data were provided by the local water authorities (Fig. 1). The series length covered the period between 1963 and 2002, and for some years there were either few or no records. Observed daily discharge was used to calculate monthly values for model

Table 2
Soil classes and average properties of the profiles present in the study area.

Soil orders	Soil taxonomy	Depth (m)	Texture	Moist bulk density (gr/cm³)	Available water capacity (mm H₂O/mm soil)	Area (%)
Alfisols	Mollic Natraqualfs	0.6	Silt loam to silty clay loam	1.36	0.18	0.097
	Typic Natraqualfs	1.2	Silt loam to silty clay loam	1.36	0.16	0.7
Mollisols	Vertic Argiaquolls	1.8	Silt loam to Silt	1.47	0.20	0.2
	Abruptic Argiudolls	2.0	Silt loam to silty clay	1.27	0.16	2.8
	Aquic Argiudolls	1.6	Silt loam to silty clay	1.35	0.17	1.7
	Typic Argiudolls	2.0	Loam	1.29	0.15	75.5
	Vertic Argiudolls	2.0	Silty clay loam	1.33	0.17	0.007
	Acuic Hapludolls	1.2	Sandy loam to Loam	1.53	0.13	0.091
	Typic Hapludolls	1.4	Sandy loam to Loam	1.51	0.13	5.8
	Typic Natralbolls	1.6	Silt loam	1.37	0.17	0.7
	Typic Paleudolls	2.5	Silt loam to silty clay loam	1.36	0.18	1.8
Not classified	Complex undifferentiated	–	–	–	–	9.7
	Water	–	–	–	–	0.104
	Miscellaneous	–	–	–	–	0.8
	Rock	–	–	–	–	0.002

Table 3
An example of a corn–wheat–soybean rotation practice.

Year	Management operation	Crop	Month	Day
1	Tillage operation		September	10
1	Planting/beginning of growing season	Corn	October	15
2	Harvest and kill operation		April	15
2	Tillage operation		June	5
2	Planting/beginning of growing season	Wheat	July	15
2	Harvest and kill operation		November	14
2	Tillage operation		December	1
2	Planting/beginning of growing season	Soybean	January	10
3	Harvest and kill operation		April	26
3	Tillage operation		April	30
3	Planting/beginning of growing season	Pasture	May	5
3	Harvest only operation		August	15

calibration (1975–1992) and validation (1993–2002), though, all those months with less than 60% of daily observations were discarded.

The initial selection of parameters to be calibrated was based on sensitivity analysis using the method known as one-at-a-time (Abbaspour et al., 2007, Schuol et al., 2008). Next, a second selection was determined by implementing global sensitivity analysis (Abbaspour et al., 2004) after the fourth iteration. Global sensitivity analysis shows the behaviour of each parameter regarding the objective function, while all other parameters are changing. Likewise, parameters are ranked according to their sensitivities, and highly correlated parameters are identified. Abbaspour et al. (2004), suggest that among the highly correlated parameters, those with the smaller sensitivities should be fixed to their best estimates and removed from additional sampling rounds.

The range of calibration parameters was initially wide, and it changed according to new values suggested by objective functions. Calibration addressed the whole basin, so that parameters were changed simultaneously for all sub-basins. Some parameters were modified by substituting a value for another (v_x), while in situations in which the parameters differed among HRUs, we chose either to decrease it or increase it by adding a value (a_x) or multiplying a value (1 ± a percentage) (r_x). Further, groundwater and main channel parameters were distributed in three areas, according to NDVI regionalisation made by Havrylenko (2013) in the basin. The regionalisation referred to had resulted in 4 groups: 2 groups of sub-basins located at the head and at the outlet of the basin (area I: 1, 2, 3, 4, 5, 6, 7 and area II: 20, 18, 12) (Fig. 4); and other 2 groups of sub-basins located in the middle part, which, in this case, were joined in a single area with similar characteristics (area III: 8, 9, 10, 11, 13, 14, 15, 16,17, 19) (Fig. 4). Next, a multi-objective formulation (Abbaspour et al., 2004) was applied using Nash–Sutcliffe coefficient (NS), and summation form of the square

error (sum). Additionally, the coefficient of determination (R^2), Nash–Sutcliffe coefficient (NS), the percent bias (PBIAS) and the ratio of the root mean square error to the observation standard deviation (RSR) were used as performance metrics. Afterwards, the uncertainty was determined for all variables of the objective function by applying Latin Hypercube sampling (Abbaspour et al., 2007).

Goodness of fit was assessed by the uncertainty measures calculated from the percentage of measured data bracketed by the 95% prediction uncertainty (95PPU). P-factor, which is the percentage of measured data bracketed by 95PPU, was calculated at 2.5% and 97.5% levels of the cumulative distribution of an output variable obtained through Latin hypercube sampling, disallowing 5% of the worst simulations. The degree of uncertainty was assessed using the R-factor, which is the average distance between the upper and the lower 95PPU (Abbaspour et al., 2004, 2007). The ideal outcome is that 100% of the measurements are bracketed by the 95PPU (P-Factor → 1) into the narrowest 95PPU band (R-Factor → 0).

2.5. Acquisition of time series of soil water content

After calibrating and validating the model, time series of SWC for the period (1982–1998) were extracted from the SWAT model at the sub-basin level and considered the entire soil profile. These data were filtered by calculating the standardised anomaly to characterise water deficit/excess more accurately, so that aSWC could be related to SPI and NDVI. Negative anomaly values mentioned above mean that aSWC is lower than the mean value, whereas positive values indicate the opposite. The equation used to calculate the standardised anomaly was Eq. (1):

$$aSWC = \frac{xi - x}{St} \tag{1}$$

where: xi is the simulated value of SWC in a given month, x is the averaged value of the time series, and St is the standard deviation.

2.6. Correlation between aSWC and SPI/aNDVI

The occurrence of water deficit/excess was determined using the severity categories of SPI established by Lloyd-Hughes and Saunders (2002). SPI was calculated applying SPI SL 6 software, developed by the National Drought Mitigation Center (NDMC), which can be downloaded from http://drought.unl.edu/MonitoringTools.aspx. SPI was calculated for the two weather stations available (between 1982 and 1998) and at one-month and three-month level. The one-month

Table 4
Initial selection of parameters to be calibrated in SWAT.

Parameter group	Parameter	Definition
Evapotranspiration	ESCO	Soil evaporation compensation factor.
	CNCOEF	Plant ET curve number coefficient
Surface runoff and time of concentration	SURLAG	Surface runoff lag coefficient.
	CN2	SCS runoff curve number for moisture condition II.
	CH_N1	Manning's value for the tributary channels.
	SLSUBBSN	Average slope length (m).
Transmission losses from surface runoff	CH_K (1)	Effective hydraulic conductivity in tributary channel alluvium (mm/h).
Soil water	SOL_AWC	Available water capacity of soil layer (mm H_2O/mm).
Lateral flow	LAT_TTIME	Lateral flow travel time (days).
	SLSOIL	Slope length for lateral subsurface flow (m).
Groundwater	GW_DELAY	Groundwater delay time (days).
	ALPHA_BF	Baseflow alpha factor (1/day).
	GWQMN	Threshold depth of water in the shallow aquifer required for return flow to occur (mm H_2O).
	GW_REVAP	Groundwater revap coefficient
	REVAPMN	Threshold depth of water in the shallow aquifer for revap or percolation to the deep aquifer to occur (mm H_2O).
	RCHRG_DP	Deep aquifer percolation fraction
Chanel water routing	TRNSRCH	Fraction of transmission losses from main channel that enter deep aquifer.
	CH_N (2)	Manning's "n" value for main channel
	CH_K (2)	Effective hydraulic conductivity in main channel alluvium (mm/h).

Table 5
SWAT model parameters included in the calibration procedure, default range, final values, and rank.

Parameter	Initial range	Basin Final value	Area I Final value	Area II Final value	Area III Final value	Final rank
ESCO (v_)	0.6–1.0	0.91	–	–	–	2
CNCOEF (v_)	0.5–1.5	0.73	–	–	–	4
SURLAG (v_)	0.05–15	0.14	–	–	–	1
CN2 (r_)	−0.1–0.1	–	−0.077	0.035	−0.08	3
CH_N1 (v_)	0.010–0.020	0.017	–	–	–	12
SLSUBBSN (v_)	70–120	66	–	–	–	13
CH_K (1) (v_)	1–50	23	–	–	–	18
SOL_AWC (r_)	−0.1–0.1	–	−0.15	0.00	0.04	14
LAT_TTIME (v_)	60–120	51	–	–	–	19
SLSOIL (v_)	50–110	75	–	–	–	17
GW_DELAY (v_)	60–120	–	37	128	96	9
ALPHA_BF (v_)	0.06–0.2	–	0.19	0.17	0.14	15
GWQMN (v_)	0–5000	–	4595	406	1502	6
GW_REVAP (v_)	0.02–0.20	–	0.10	0.13	0.02	11
REVAPMN	0–500	–	294	448	455	16
RCHRG_DP	0–1	–	0.47	0.37	0.2	10
TRNSRCH (v_)	0.0–1.0	0.56	–	–	–	5
CH_N (2) (v_)	0.010–0.050	–	0.021	0.017	0.026	7
CH_K (2) (v_)	30–100	–	41	32	88	8

SPI reflects relatively short-term conditions, so that its application can be closely related to short-term soil moisture and crop stress, especially during the growing season. A three-month SPI reflects short- and medium-term moisture conditions. In primary agricultural regions, the three-month SPI might be applicable to highlight available moisture conditions.

NDVI index (Tarpley et al., 1984) was chosen because it has been successfully used to identify and track areas affected by droughts at regional and local levels (Seiler et al., 2000; Tucker and Anyamba, 2005; Bayarjargal et al., 2006; Bajgirana et al., 2008). In addition, NDVI may be used to indicate conditions and variations of vegetative health at any given time of the vegetation, ranging between −1 and 1. Positive values of NDVI between 0.1 and 0.7 represent vegetated areas, so that high values of NDVI mean increases in vegetation or vegetation with great vigour. In contrast, negative values are interpreted as non-vegetated areas such as water, ice and snow bodies, while values close to 0 represent areas of bare soil. We used the set of fortnightly images of NDVI, which correspond to the AVHRR sensor from the National Oceanic and Atmospheric Administration and were provided for free by the Global Inventory Monitoring and Modelling Systems http://glcf.umiacs.umd.edu/data/gimms/. The original data were downloaded with the radiometric corrections to be used from a multitemporal point of view.

To apply this index, each fortnightly image was averaged monthly (for the period 1982–1998 and every sub-basin) by raster/vector layer operations. A mean monthly value for each sub-basin was obtained. The analysis of the temporal variation was based on studying the monthly evolution by using graphs aimed to detect periods with low NDVI values, as well as their duration. Similarly to SWC, NDVI values were filtered using the standardised anomaly (aNDVI). The resulting values were interpreted as follows: negative values indicated a response lower than normal, whereas positive values showed the opposite.

To explore the statistical relationship between monthly values of SPI/aNDVI and aSWC, the Pearson correlation coefficient (McNemar, 1969) (at a 5% significance level) and the bivariate correlation method (McCuen, 2002) were used.

3. Results

3.1. Model calibration and validation

The calibration process began including 30 hydrological parameters, after the fourth iteration 19 were found to be sensitive to discharge (Table 4). The list of chosen parameters, the initial and optimised values, and the relative sensitive ranking are shown in Table 5. Moreover, the results of objective functions to reach the optimisation are listed in Table 6. In general, monthly calibration offered reasonably satisfactory results. It was necessary to carry out 20 iterations of 400 simulations each one to achieve the final optimisation. Goodness of fit of the monthly calibration was evaluated by estimating the uncertainty (Fig. 5). In this regard, acceptable values of the P- and R-factors were obtained (Table 6). Likewise, the validation results were also satisfactory (Fig. 6); the metric performance for the model in the validation can be seen in Table 6.

3.2. Correlation and analysis of temporal variation between aSWC and aNDVI/SPI

Correlation between monthly values of aSWC and one-month SPI/three-month SPI was significant, although lower values were derived when one-month SPI was lagged one month (Fig. 7A). In addition, higher correlations were obtained when three-month SPI was considered (Fig. 7B). A seasonal pattern, associated with the growing season of crops, was detected. Higher values of correlation were found between October and March (0.64 ≤ r ≤ 0.83) when three-month SPI was taken into account.

The correlation between monthly values of aSWC and aNDVI also showed a seasonal pattern (Fig. 8), although r values were less significant than those derived from correlating aSWC with SPI. Regarding the above, higher values of correlation were obtained, when aNDVI was lagged one month, mainly between October and March, when r values were between 0.26 and 0.45 (Fig. 8B).

Table 6
Final statistic coefficients for calibration and validation procedures.

Objective function	Stage	R2	NS	PBIAS	RSR	P-factor	R-factor
Nash–Sutcliffe coefficient (NS)	Calibration	0.70	0.59	14.1	0.64	0.66	0.83
	Validation	0.76	0.75	10.1	0.50	0.67	0.46
Summation form of the square error (SUM)	Calibration	0.70	0.59	14.1	0.64	0.68	0.87
	Validation	0.76	0.75	10.1	0.50	0.77	0.64
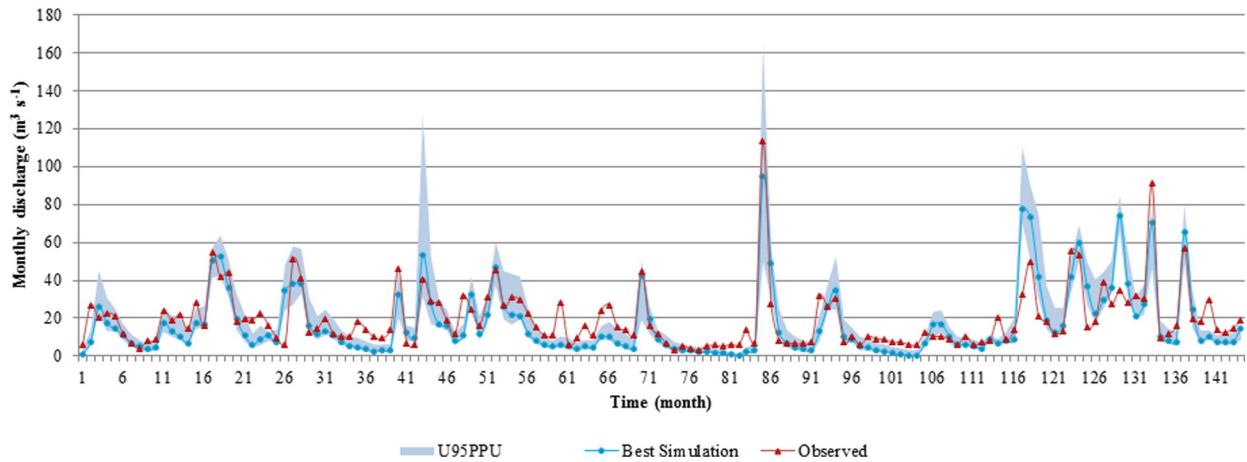
Fig. 5. Monthly calibration between January 1979 and December 1992 (including missing data). The graph shows the 95% prediction uncertainty intervals along with the measured discharge.

The analysis of the temporal variability of aSWC and SPI/aNDVI resulted in the observation that aSWC follows the pattern given by precipitation and therefore by SPI. The aSWC curve showed a relatively smooth response regarding the SPI peaks (Fig. 9). So, if a dry period occurs, aSWC curve remains above the curve of three-month SPI (except in severe droughts), whereas if a wet period occurs, but the antecedent conditions were fairly normal, the aSWC curve is fitted or slightly below the three-month SPI curve (except in very wet situations). However, similar results to aSWC–SPI were not observed between aSWC and aNDVI (Fig. 10), and aNDVI did not follow the expected pattern in severe situations (wet or dry events).

4. Discussion

The methodological approach used here allowed obtaining a long-term record of SWC, which was tested establishing the correlation between aSWC and aNDVI/SPI. The results obtained as well as the methodology used are novel in the context of Argentina, as a hydrological model combined with the SPI/NDVI indices is used to estimate SWC for the first time.

According to Moriasi et al. (2007), the values obtained for the objective functions considered indicate a satisfactory performance of the model. Likewise, they are consistent with those obtained by other authors in similar geographic contexts and with a shortage of data (Richard et al., 2010; Barrios and Urribarri, 2010; Gonzalez, 2011; Jha, 2012). The calibration and validation of the SWAT model was conditioned by the spatial representativeness of the precipitation and flow data. There is only one gauging station available, and in the basin and its surroundings there are only two weather stations. As a result, calibration was done only in the control section that coincided with the outlet of the basin. Therefore, calibration may be forced, so that the matching of the parameters can be achieved using ranges for them without enough physical sense. In addition, this circumstance can lead to errors in the characterisation of the processes that determine the transformation of rainfall into runoff. Thus, it would be desirable to have several gauging stations in the basin or at least one with a long time series (Abbaspour et al., 2007). The shortage of hydro-meteorological data, mainly rainfall (the most sensitive in this respect), implied a higher uncertainty of estimates concerning average values of monthly accumulated rainfall, especially in times of flooding in which hydrological simulations can lead to an underestimation of flows.

SPI results are similar to those found by Núñez et al. (2005) and Gonzalez and Cariaga (2009), who concluded that the SPI index is suitable to identify and follow dry and humid events in the humid Pampas. Furthermore, the moving average analysis showed that severe droughts identified with the three-month SPI could have a cyclic behaviour. Regarding the correlations between aNDVI/SPI and aSWC, significant and positive correlations were found between SPI and aSWC, whereas correlations between aNDVI and aSWC showed lower values. Likewise, a seasonal pattern was noted in the response of both indices.

Correlation between aSWC and three-month SPI showed a lower dispersion and a more marked seasonal pattern than one-month SPI (Fig. 7). Moreover, the seasonal pattern showed that the best correlations
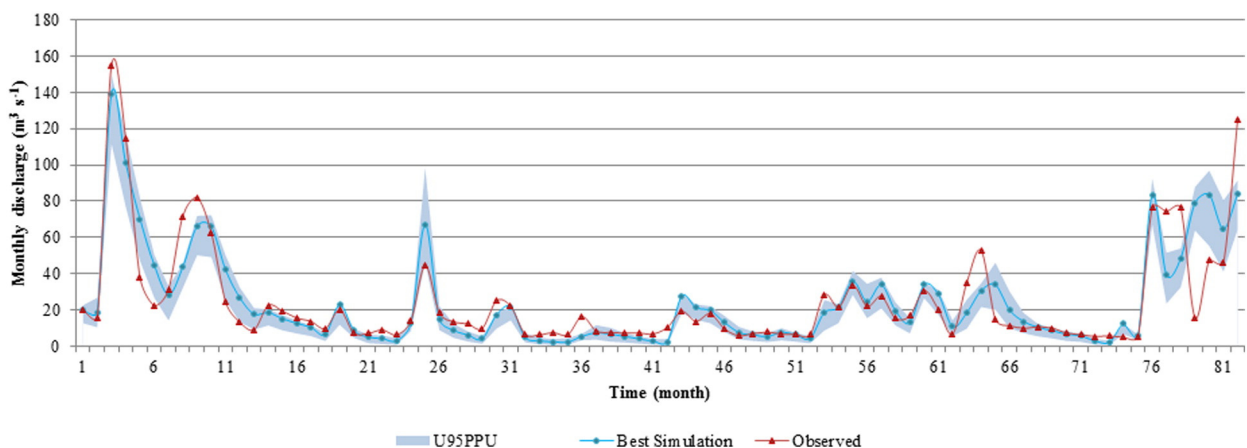
Fig. 6. Monthly validation between January 1993 and December 1998 (including missing data). The graph shows the 95% prediction uncertainty intervals along with the measured discharge.
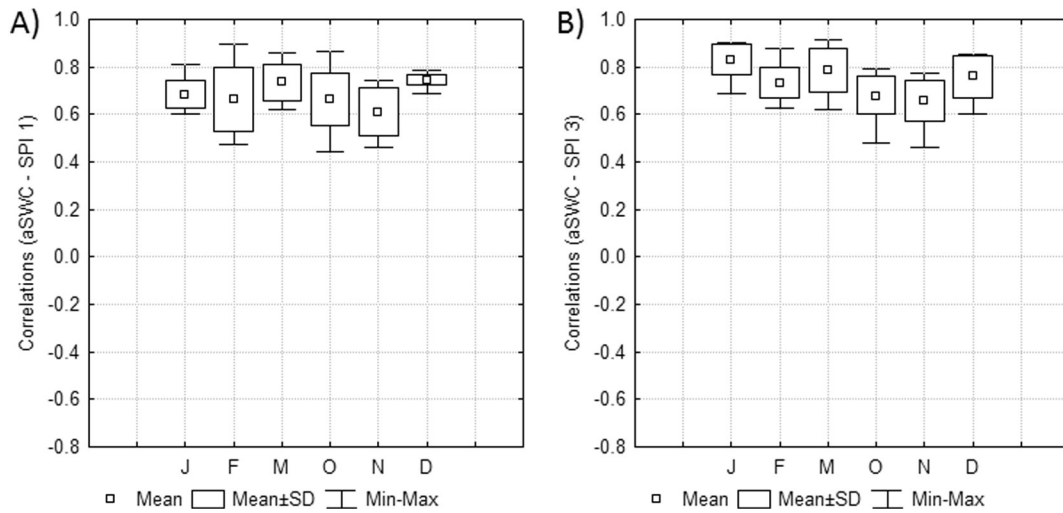
Fig. 7. Box plots of the result of the correlation between aSWC and SPI, including all subbasins in each month. A) aSWC and SPI (one-month), B) aSWC and SPI (three-month).

occur in rainy season with high SWC. These results are consistent with those obtained by Richard et al. (2010) in similar phenological periods to the one considered here. Hence, the result shows that there is no direct relationship between precipitation and SWC and it indicates that three-month SPI has a short delay and a cumulative effect of precipitation on SWC. One of the main reasons is related to the physical characteristics of the soils and their local conditions (e.g. topographic factors), while the low and variable correlations in dry months may be due to the fact that SWC responds to changes in precipitation in dry months with a lag.

Concerning correlations between aNDVI and aSWC, higher values were obtained when the aNDVI was lagging one month in regards to SWC. This result shows that crops respond to change in precipitation, but this change is not instantaneous and has a cumulative effect on vegetation. The lowest values were obtained at the beginning or at the end of the growth phase of crops. This is consistent with the observation made by Narasimhan (2004) and Richard et al. (2010), who suggested that correlations have to be established only for the growth period. Another issue to be considered is that the correlation also depends on the depths of the root system of the crops. Most of the pasture and agriculture crops have shallow root systems and use only the SWC available in the first part of the soil profile (Narasimhan and Srinivasan, 2005). Consequently, these results can be partially explained by the fact that SWAT estimates SWC in the whole edaphic profile and, therefore, below the depth reached by the actual root system. Wang et al. (2007) and

Schnur et al. (2010) analysed the response between soil moisture at different depths of the roots and NDVI, finding that they are closely related. These authors also found that the NDVI corresponding to vegetation with short root systems presents positive and significant correlations with SWC in the first centimetres of the soil, and that values decrease and have a larger lag at higher depths. Conversely, in areas with species with deeper root systems correlations increased with depth.

In addition, between April and September, aNDVI followed an erratic pattern, which showed differences with the aSWC time series (Fig. 10). This could be associated with the fact that the system becomes more variable. This means that as crops mature and are harvested, the mean value of aNDVI obtained for each sub-basin no longer reflects just the state of the vegetation, but also a mosaic of parcels with mature crops, bare soils, and newly planted or harvested crops. Another situation perceived during some droughts is that a rainfall event (only detected with one-month SPI) positively increases the aNDVI curve without significant increases in the soil moisture curve.

Thus, many factors may cause the low level of significance in correlations between aNDVI and aSWC, such as spectral bandwidth, radiometric and spatial resolution of AVHRR instrument, from which NDVI is derived, spatial scale at which NDVI was used, land cover or the variability of some local conditions (i.e. type and depth of soil, water table height, antecedent moisture conditions, slope, and homogeneity of the sub-basin with respect to land use). In this regard, Richard et al. (2010)
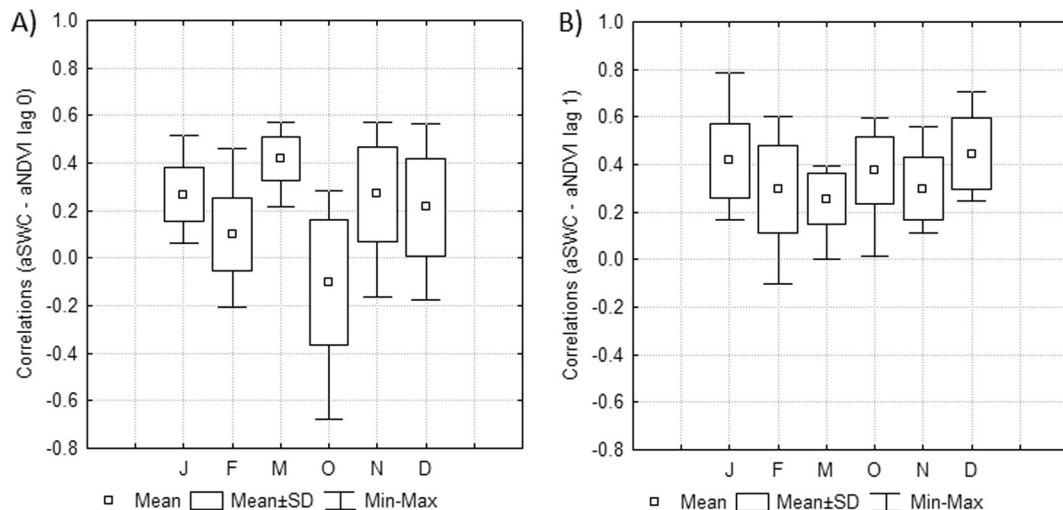
Fig. 8. Box plots of the result of the correlation between aSWC and aNDVI, including all subbasins in each month. A), aSWC and aNDVI, B) aSWC and aNDVI (lagged 1 month).
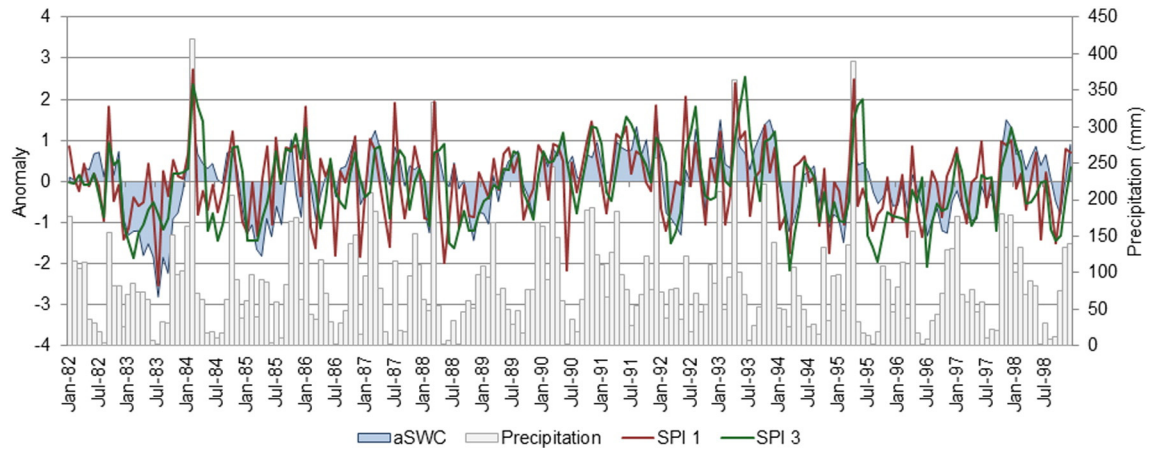
Fig. 9. Monthly evolution of aSWC, one-month/three-month SPI and precipitation between 1982 and 1998.

analysed the correlation between NDVI and soil moisture at sites with different soil and climatic characteristics, and concluded that both the vegetation and soil properties play key roles in the ability of NDVI to represent the role of SWC. In Arrecifes basin, dominant soils are Typic Argiudolls, but the presence of other soil types with local connotation could cause different responses in vegetation. Havrylenko (2013) analysed the spatial variability of NDVI in the basin, applying principal components method across the study area. Four sub-basin groups were found which could be associated to the type of soils present. On the one hand, 2 groups of sub-basins located at the head and at the outlet of the basin were related to hydromorphic and poorly drained soils; and, on the other hand, 2 groups of sub-basins located in the middle part of the basin were linked to deep and well drained soils. So, it is likely that these latter areas will be more vulnerable to agricultural drought in dry periods.

It is interesting to compare the evolution of SWC with respect to SPI and NDVI curves. Analysing drought in time series-plot allowed observing the performance of drought events occurred in 1988/89, 1994/95 and 1995/96. These three events were major droughts at Pampas region level; the process began with dry winters and continued with insufficient rainfall until the next summer. The three-month SPI curve indicated intense droughts until around February; the one-month SPI curve showed a fluctuating pattern according to the monthly precipitation fallen; and the aSWC curve reflected negative values below mean value in 1988/89 and 1994/95, and negative values close to mean value in 1995/96 (Fig. 9). However, the anomalous behaviour of SWC curve between spring of 1995 and summer of 1996 was due to the fact that the model was influenced by the extreme events of precipitation occurred in the autumn of 1995. Moreover, the aNDVI curve

showed negative values below mean value in 1988/89, positive values above mean value in 1994/95, and values fluctuating around the mean in 1995/96 (Fig. 10).

The methodology had limitations that did not allow for an optimal evaluation of the suitability of SWAT in the estimation of SWC. Nonetheless, the methodology could be applied with less uncertainty with appropriate parameterization of SWAT and better results could be obtained in processes related to the hydrological cycle such as the one studied here. Thus, the approach implemented here could be used by decision makers to improve the management of agricultural resources in Argentina, because SWC is the most direct and important indicator of agricultural drought (Nam et al., 2012). Once the methodology is set, the combined use of SWC derived from SWAT and different drought indices could determine the onset, severity, spatial extent, and end of drought conditions.

5. Conclusions

For the first time in Argentina, a continuous monthly record of SWC was obtained in a region with shortage of data regarding hydrometeorology, land use and topography. The reliability of simulated SWC derived from SWAT was tested establishing the correlation between this parameter and aNDVI/SPI indices. Objective functions used during the calibration and validation of the SWAT model defined reasonably satisfactory values, although they could be improved with increasing availability of precipitation and flow data. Moreover, positive and significant correlations were obtained between aSWC and one/three-month SPI. It is considered that three-month SPI is a suitable index for the study of agricultural drought
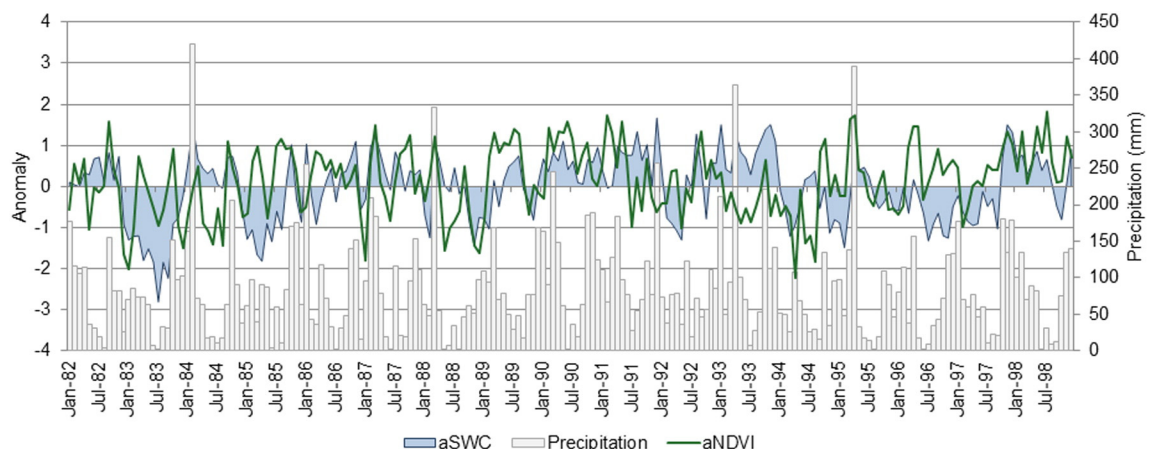
Fig. 10. Monthly evolution of aSWC, aNDVI and precipitation between 1982 and 1998.

for short-term weather conditions. In addition, SPI provided information about degree and magnitude of events. However, the statistical relationship between aSWC and aNDVI was less significant. Thus, it is considered that the NDVI index should be used with caution, since it is strongly conditioned by the depth of the root system, the variability of some local conditions, as well as by the occurrence of short and intense precipitation events within a drought context. Besides, further research is needed to better characterise the factors affecting NDVI values and their relationships with SWC. Although further testing should be carried out about the confidence of the SWAT simulation of SWC with other drought indices, it has currently obtained promising results. It is considered that the SWAT model combined with drought index could be used as agricultural drought monitoring tools and early warning systems at basin scale. It is difficult to know when agricultural droughts begin and end, just as it is difficult to know the magnitude of the impact they could have on crops and their spatial extension. Thus, because of its high variability in space and time, knowledge of SWC is generally inaccurate. For this reason, a calibrated SWAT model can be applied to obtain SWC time series and its spatial distribution both in Arrecifes basin and other watersheds of the Pampas region. Thereby, the results obtained have important implications at management level, as they could allow decision makers to know the spatial and temporal variability of agricultural droughts and thus support a risk-based decision-making process.

Acknowledgements

References

Abbaspour, K., Johnson, C., van Genuchten, M., 2004. Estimating uncertain flow and transport parameters using a sequential uncertainty fitting procedure. Vadose Zone J. 3 (4), 1340–1352.

Abbaspour, K., Yang, J., Maximov, I., Siber, R., Bogner, K., Mieleitner, J., Zobrist, J., Srinivasan, R., 2007. Modelling hydrology and water quality in the pre-ailpine/alpine Thur watershed using SWAT. J. Hydrol. 333 (2–4), 413–430.

Arnold, J.G., Fohrer, N., 2005. SWAT 2000: current capabilities and research opportunities in applied watershed modelling. Hydrol. Process. 19 (3), 563–572.

Arnold, J.G., Kiniry, J.R., Srinivasan, R., Williams, J.R., Haney, E.B., Neitsch, S.L., 2011. Soil and water assessment tool input/output file documentation version 2009. Technical report No 365 [online]. Blackland Research Center, Texas Water Resources Institute, College Station, Texas (Available from: http://swat.tamu.edu/media/19754/swat-io-2009.pdf. [Verified on 10 February 2013]).

Bajgirana, P.R., Darvishsefatb, A., Khalilic, A., Makhdoum, M.F., 2008. Using AVHRR-based vegetation indices for drought monitoring in the northwest of Iran. J. Arid Environ. 72, 1086–1096.

Barrios, A.G., Urribarri, L.A., 2010. Aplicación del modelo SWAT en los Andes venezolanos: Cuenca alta del río Chama. Rev. Geogr. Venez. 51 (1), 11–29.

Bayarjargal, Y., Karnieli, A., Bayasgalan, M., Khudulmur, S., Gandush, C., Tucker, C.J., 2006. A comparative study of NOAA–AVHRR derived drought indices using change vector analysis. Remote Sens. Environ. 105, 9–22.

Bergström, S., 1995. The HBV model. In: Singh, V.P. (Ed.), Computer Models of Watershed Hydrology. Water Resources Publications, Highlands Ranch, pp. 443–476.

Bianchi, R.A., Cravero, S.A., 2010. Atlas climático digital de la República Argentina. Ediciones INTA, Salta, Argentina, p. 84.

Blaschke, T., 2010. Object based image analysis for remote sensing. ISPRS J. Photogramm. Remote Sens. 65 (1), 2–16.

Conover, W.J., 1999. Practical Nonparametric Statistics. 3rd ed. John Wiley & Sons, New York, p. 584.

Das, H.P., Adamenko, T.I., Anaman, K.A., Gommes, R.G., Johnson, G., 2003. Agrometeorology related to extreme events. Technical Note 201. WMO No 943: Geneva, p. 152.

Di Luzio, M., Arnold, J.G., 2004. Formulation of a hybrid calibration approach for a physically based distributed model with NEXRAD data input. J. Hydrol. 298 (1–4), 136–154.

Farr, T., Rosen, P., Caro, E., Crippen, R., Duren, R., Hensley, S., Kobrick, M., Paller, M., Rodriguez, E., Roth, L., Seal, D., Shaffer, S., Shimada, J., Umland, J., Werner, M., Oskin, M., Burbank, D., Alsdorf, D., 2007. The shuttle radar topography mission. Rev. Geophys. 45, RG2004http://dx.doi.org/10.1029/2005RG000183.

Gonzalez, L., 2011. Modelización hidrológica del río Odiel: aplicación al estudio de la contaminación por drenaje ácido de minas. Universidad de Huelva, Thesis (PhD).

Gonzalez, M., Cariaga, M., 2009. An approach to seasonal forecasting of summer rainfall in Buenos Aires, Argentina. Atmosfera 22 (3), 265–279.

Grayson, R.B., Western, A.W., Chiew, F.H.S., Blöschl, G., 1997. Preferred states in spatial soil moisture patterns: local and non-local controls. Water Resour. Res. 33 (12), 2897–2908.

Haack, B., Jampoler, S., 1995. Colour composite comparisons for agricultural assessments. Int. J. Remote Sens. 16, 1589–1598.

Han, E., Merwade, V., Heathman, G., 2012. Implementation of surface soil moisture data assimilation with watershed scale distributed hydrological model. J. Hydrol. 416, 98–117.

Hartmann, T., Di Bella, C., Oricchio, P., 2003. Assessment of the possible drought impact on farm production in the SE of the province of Buenos Aires, Argentina. ISPRS J. Photogramm. Remote Sens. 57 (4), 281–288.

Havrylenko, S., 2013. Caracterización de sequías en cuencas agrícolas de la región pampeana mediante la aplicación del modelo hidrológico SWAT. Master Thesis. El Litoral National University, Santa Fe, Argentina.

Hirsch, R.M., Slack, J.R., Smith, R.A., 1982. Techniques of trend analysis for monthly water quality data. Water Resour. Res. 18 (1), 107–121.

Hong, W., Park, M., Park, J., Park, G., Kim, S., 2010. The spatial and temporal correlation analysis between MODIS NDVI and SWAT predicted soil moisture during forest NDVI increasing and decreasing periods. KSCE J. Civ. Eng. 14 (6), 931–939.

Horler, D.N.H., Ahern, F.J., 1986. Forestry information content of Thematic Mapper data. Int. J. Remote Sens. 7 (3), 405–428.

Instituto Nacional de Tecnología Agropecuaria (INTA), 2009. Cartas de suelos de la República Argentina – Provincia de Buenos Aires: Escala 1:50.000 [online]. Buenos Aires, Instituto de Suelos. Availablefrom: http://anterior.inta.gob.ar/f/?url=http://anterior.inta.gob.ar/suelos/ [Verifiedon 15 April 2012].

Instituto Nacional de Tecnología Agropecuaria (INTA), 2013. SIGA Sistema de Información y Gestion Agrometeorológico [online] Available from: http://siga2.inta.gov.ar/en/estadistica/ [Verified on 3 January 2012].

Instituto Nacional de Tecnología Agropecuaria y Programa de Cambio Rural (INTA-PCR), 1997m. Guía práctica para el cultivo de Girasol. Secretaría de Agricultura, Gandería, Pesca y Alimentación, INTA, Buenos Aires (220 pp.).

Instituto Nacional de Tecnología Agropecuaria y Programa de Cambio Rural (INTA-PCR), 1997m. Guía práctica para el cultivo de Maíz. SAGPyA, INTA, Buenos Aires (220 pp.).

Instituto Nacional de Tecnología Agropecuaria y Programa de Cambio Rural (INTA-PCR), 1997m. Guía práctica para el cultivo de Soja. SAGPyA, INTA, Buenos Aires Buenos Aires (243 pp.).

Instituto Nacional de Tecnología Agropecuaria y Programa de Cambio Rural (INTA-PCR), 1997m. Guía práctica para el cultivo de Trigo. SAGPyA, INTA, Buenos Aires (182 pp.).

Jha, M.K., 2012. Quantifying soil moisture distribution at a watershed scale. In: Hernandez-Soriano, M. (Ed.), Soil Health and Land Use Management http://dx.doi.org/10.5772/29990.

Johnson, G., Qian, Y., Davis, J., 2009. Topdressing Kentucky bluegrass with compost increases soil water content and improves turf quality during drought. Compost Sci. Util. 17 (2), 95–102.

Klawitter, A., 2006. A modelling concept for the integrative analysis of urban and rural hydrology on river basin scale (in German). Publication series of the Institute of Hydraulic and Water Resources Engineering 138.

Li, M., Ma, Z., Du, J., 2010. Regional soil moisture simulation for Shaanxi Province using SWAT model validation and trend analysis. Sci. China Earth Sci. 53 (4), 575–590.

Liang, X., Wood, E.F., Lettenmaier, D.P., 1996. Surface soilmoistureparametrization of the VIC-2L model: evaluation and modification. Glob. Planet. Chang. 13 (1–4), 195–206.

Llano, M.P., Penalba, O.C., 2010. A climatic analysis of dry sequences in Argentina. Int. J. Climatol. 31, 504–513.

Lloyd-Hughes, B., Saunders, M., 2002. A drought climatology for Europe. Int. J. Climatol. 22, 1571–1592.

Maltese, A., Bates, P., Capodici, F., Cannarozzo, M., Ciraolo, G., La Loggia, G., 2013. Critical analysis of thermal inertia approaches for surface soil water content retrieval. Hydrol. Sci. J. 58 (5), 1144–1161.

Mavi, S.H., Tupper, G.J., 2004. Agrometeorology: Principles and Applications of Climate Studies in Agriculture. Haworth Press, New York, p. 364.

McCuen, R., 2002. Modeling Hydrologic Change: Statistical Methods. CRC Press LLC, Boca Raton, Florida, p. 433.

McKee, T.B., Doesken, N.J., Kleist, J., 1993. The relationship of drought frequency and duration to time scales. Eighth Conf. on Applied Climatology, Anaheim, CA, Amer. Meteor. Soc., pp. 179–184

McNemar, Q., 1969. Psychological Statistics. 4th ed. John Wiley & Sons, New York.

Mishra, A., Singh, V., Desai, V., 2009. Drought characterization: a probabilistic approach. Stoch. Env. Res. Risk A. 23 (1), 41–55.

Moriasi, D., Arnold, J., Van liew, M., Bingner, R., Harmel, R., Veith, T., 2007. Model evaluation guidelines for systematic quantification of accuracy in watershed simulations. Trans. ASABE 50 (3), 885–900.

Nam, W., Choi, J., Yoo, S., Jang, M., 2012. A decision support system for agricultural drought management using risk assessment. Paddy Water Environ. 10 (3), 197–207.

Narasimhan, B., 2004. Development of Indices for Agricultural Drought Monitoring Using a Spatially Distributed Hydrologic Model Thesis (PhD) Texas A&M University.

Narasimhan, B., Srinivasan, R., 2005. Development and evaluation of Soil Moisture Deficit Index (SMDI) and Evapotranspiration Deficit Index (ETDI) for agricultural drought monitoring. Agric. For. Meteorol. 133 (1–4), 69–88.

Narasimhan, B., Srinivasan, R., Arnold, J., Di Luzio, M., 2005. Estimation of long-term soil moisture using a distributed parameter hydrologic model and verification using remotely sensed data. Trans. ASAE 48 (3), 1101–1113.

Neitsch, S.L., Arnold, J.G., Kiniry, J.R., Williams, J.R., 2011. Soil and water assessment tool. Theoretical documentation: version 2009. Technical report N° 406 [online]. Texas Water Resources Institute, Texas A&M University, College Station, Texas, p. 647 Available from: http://swat.tamu.edu/documentation/ [Verified on 10 February 2012].

Núñez, S., Núñez, L., Podestá, G., Skansi, M., 2005. El índice estandarizado de precipitación como herramienta para la caracterización y el concepto de la sequía: una prueba de concepto [online]. 9th Argentine Congress of Meteorology.3–7 October 2005 Buenos Aires. Centro Argentino de Meteorólogos (Available from: https://www.rsmas.miami.edu/users/agriculture/pubs/meetings/abstracts/SPI-SMN.pdf [Verified on 8 February 2012]).

Olivera, F., Maidment, D., 1999. Geographic Information Systems (GIS)-based spatially distributed model for runoff routing. Water Resour. Res. 35 (4), 1155–1164.

Peel, M.C., Finlayson, B.L., McMahon, T.A., 2007. Up dated world map of the Köppen–Geiger climate classification. Hydrol. Earth Syst. Sci. 11, 1633–1644.

Platt, R.V., Rapoza, L., 2008. An evaluation of an object-oriented paradigm for land use/land cover classification. Prof. Geogr. 60 (1), 87–100.

Priestley, C.H.B., Taylor, R.J., 1972. On the assessment of the surface heat flux and evaporation using large-scale parameters. Mon. Weather Rev. 100, 81–92.

Ravelo, A.C., Da Porta, W.A., Zanvettor, R.E., 1999. Evaluación de las sequías extremas en la región pampeana argentinadurante el período 1930–1990. XI Congreso Brasileiro de Agrometeorología, II Reunión Latino-Americana de Agrometeorología. Florianopolis, SC Brasil, 19 to 22 July 1999.

Richard, J., Madramootoo, C., Trotman, A., 2010. The development of the SPI and NDVI for 3 study sites in Jamaica, with an investigation into their use in understanding soil water during water stressed conditions in Jamaica. XVIIth World Congress of the International Commission of Agricultural and Biosystems Engineering (CIGR), 13–17 June 2010. Canadian Society for Bioengineering, Quebec (Available from: http://www.mcgill.ca/files/cariwin/CEF2010_Richards_SPI_NDVI_paper.pdf [Accessible 15 June 2013]).

Saxton, K.E., Rawls, W.J., 2006. Soil water characteristic estimates by texture and organic matter for hydrologic solutions. Soil Sci. Soc. Am. J. 70, 1569–1578.

Schnur, M., Xie, H., Wang, X., 2010. Estimating root zone soil moisture at distant sites using MODIS NDVI and EVI in a semi-arid region of southwestern USA. Ecol. Inform. 5 (5), 400–409.

Schuol, J., Abbaspour, K.C., Srinivasan, R., Yang, H., 2008. Estimation of freshwater availability in the West African sub-continent using the SWAT hydrologic model. J. Hydrol. 352, 30–49.

Seiler, R.A., Rotondo, V., 2006. Las sequías en los últimos veinte años en el sur de Córdoba evaluadas mediante el índice estandarizado de precipitación. XII Reunión Científica de Argentina de Agrometerorología. 5–8 September 2006. La Plata, Buenos Aires, Argentina.

Seiler, R.A., Kogan, F., Sullivan, J., 1998. AVHRR-based vegetation and temperature condition indices for drought detection in Argentina. Adv. Space Res. 21 (3), 481–484.

Seiler, R.A., Kogan, F., We, G., 2000. Monitoring weather impact and crop yield from NOAA-AVHRR data in Argentina. Adv. Space Res. 26 (7), 1177–1185.

Soil Survey Staff, 2014. Keys to Soil Taxonomy. 12th ed. USDA-Natural Resources Conservation Service, Washington DC, p. 360.

Susaki, J., 2012. Segmentation of shadowed buildings in dense urban areas from aerial photographs. Remote Sens. 4 (4), 911–933.

Tarpley, J., Schneider, S., Money, R., 1984. Global vegetation indices from NOAA-7 meteorological satellite. J. Appl. Meteorol. 23, 491–494.

Tucker, C.J., Anyamba, A., 2005. Analysis of Sahelian vegetation dynamics using NOAA–AVHRR NDVI data from 1981–2003. J. Arid Environ. 63, 596–614.

Van Lanen, H., Wanders, N., Tallaksen, L., Van Loon, A., 2013. Hydrological drought across the world: impact of climate and physical catchment structure. Hydrol. Earth Syst. Sci. 17 (5), 1715–1732.

Viglizzo, E.F., 2008. Agricultura, clima y ambiente en Argentina: tendencias, interacciones e impactos. In: Solbrig, O., Adamoli, J. (Eds.), Agro y Ambiente: una agenda compartida para el desarrollo sustentable. Foro de la Cadena Agroindustrial Argentina, Buenos Aires, pp. 141–166.

Viglizzo, E., Lertora, F., Pordomingo, A., Bernardo, J., Roberto, Z., Del Valle, H., 2001. Ecological lessons and applications from one century of low external-input farming in the pampas of Argentina. Agric. Ecosyst. Environ. 83 (1–2), 65–81.

Wang, Z., 1990. Principles of Photogrammetry (with Remote Sensing). Press of Wuhan Technical University of Surveying and Mapping, and Publishing House of Surveying and Mapping, Beijing.

Wang, X., Xie, H., Guan, H., Zhou, X., 2007. Different responses of MODIS-derived NDVI to root-zone soil moisture in semi-arid and humid regions. J. Hydrol. 340 (1–2), 12–24.

Wang, D., Hejazi, M., Cai, X., Valocchi, A., 2011. Climate change impact on meteorological, agricultural, and hydrological drought in central Illinois. Water Resour. Res. 47, W09527. http://dx.doi.org/10.1029/2010WR009845.

Wilhite, D.A., 2005. The role of disaster preparedness in national planning with specific reference to droughts. In: Sivakumar, M.V.K., Motha, R.P., Das, H.P. (Eds.), Natural Disasters and Extreme Events in Agriculture. Springer-Verlag, Berlin, p. 370.

Wilhite, D.A., Sivakumar, M.V.K., Pulwarty, R., 2014. Managing drought risk in a changing climate: the role of national drought policy. Weather Clim. Extremes 3, 4–13.

William, J.R., 1969. Flood routing with variable travel time or variable storage coefficients. Trans. ASABE 12 (1), 0100–0103.

Xu, X., Ge, Q., Zheng, J., Dai, E., Zhang, X., He, S., Liu, G., 2013. Agricultural drought risk analysis based on three main crops in prefecture-level cities in the monsoon region of east China. Nat. Hazards 66 (2), 1257–1272.

Zhang, L., Dawes, W.R., Hatton, T.J., Reece, P.H., Beale, G., Packer, I., 1999. Estimation of soil moisture and groundwater recharge using the TOPOG_IRM model. Water Resour. Res. 35, 149–161.